RSC
Mechanochemistry

ROYAL SOCIETY
OF CHEMISTRY

PAPER

View Article Online
View Journal | View Issue

Cite this: *RSC Mechanochem.*, 2025, **2**, 573

One-pot synthesis of aldimines *via* single screw extrusion: a mechanochemical approach†

Aditya Sunil Lade, Khetal Vasant Surana, Sai Srinivas Ponugoti and Shreerang V. Joshi *

Received 7th January 2025
Accepted 10th April 2025

DOI: 10.1039/d5mr00004a

rsc.li/RSCMechanochem

We report a continuous, solvent-free method for aldimine synthesis using single-screw extrusion (SSE) that achieves high yields with water as the sole byproduct. Under optimized conditions, SSE delivered aldimines in high to near-quantitative yields (>99% for selected derivatives) across diverse substrate classes including cyclohexanol amines, L-phenylalaninate methyl esters and ethylenediamine-derived bis-aldimines without requiring product purification. Furthermore, an optimized process is demonstrated, with a throughput rate of 6740 g day^{-1}, corresponding to a space-time yield of 1716 kg m^{-3} day^{-1}. The extrusion process outperformed mechanochemical grinding and batch methods in efficiency and crystallinity, as evidenced by the DSC endothermic peak. The synthesized compounds were characterized using various analytical tools like IR, GC-MS, NMR, single crystal XRD and HRMS. By leveraging mechanochemistry in a continuous flow system, SSE provides a simple yet powerful platform that significantly expands the possibilities for sustainable organic synthesis.

Introduction

Imines, characterized by their C═N functional group, are valuable intermediates in pharmaceuticals, materials science and catalysis.[1–8] They play a crucial role in drug development,[9] advanced polymer synthesis,[10] dye production[11] and the fabrication of metal complexes[12] and nanomaterials.[13] Given their broad applications, the development of efficient and sustainable synthetic methods is an important research priority. Traditional imine synthesis involves the condensation of amines and aldehydes in organic solvents, often requiring extended reaction times, catalysts or dehydrating agents, which raise concerns about hazardous solvent use, waste generation and process inefficiency.[14]

Greener alternatives such as grinding,[15] ultrasound irradiation,[16] organocatalysis,[17] enzyme catalysis,[18] photocatalysis[19] and micellar catalysis[20] have been explored; however, their practical application is often hindered by narrow substrate compatibility and scalability limitations.

Mechanochemistry has emerged as a powerful tool for solvent-free synthesis, offering a greener and more sustainable alternative to conventional solution-based methods, utilizing mechanical energy to drive chemical reactions without the need for hazardous solvents.[21] By applying grinding, compression, or shear forces, mechanochemical methods reduce waste and energy consumption, aligning with green chemistry principles.[22]

However, significant challenges remain, particularly in reaction control, reproducibility and scalability, limiting mechanochemistry's industrial adoption.[23] Mortar-and-pestle grinding, though simple and accessible, suffers from low energy input, inconsistent mixing and poor reproducibility, often leading to incomplete reactions and prolonged processing times.[24] Planetary ball milling offers higher energy input and better mixing but introduces uncontrolled heat generation, causing temperature fluctuations, side reactions and reduced selectivity.[25] While strategies like cryomilling and thermal regulation exist, they add cost and complexity, making them impractical for large-scale use.[26] Moreover, the batch-mode operation of ball milling restricts scalability, highlighting the need for continuous mechanochemical methods better suited for industrial workflows.[27]

To overcome scalability issues, researchers have explored continuous mechanochemical techniques such as extrusion-based approaches, which offer precise reaction control, improved reproducibility and scalability. Twin-screw extrusion (TSE) has gained attention as an advanced mechanochemical method, originally developed for polymer processing,[28] pharmaceuticals[29] and the food industry.[30] Unlike batch-based methods, TSE operates continuously, enabling efficient mixing, controlled shear forces, and precise temperature regulation throughout the reaction process. This adaptability has made TSE particularly valuable for solvent-free organic synthesis,[31] including pharmaceutical co-crystals,[32] metal–organic frameworks (MOFs)[33] and deep eutectic solvents (DESs).[34] Deborah E. Crawford and coworkers reported the first imine synthesis

---

Department of Pharmaceutical Sciences and Technology, Institute of Chemical Technology, Nathalal Parekh Marg, Matunga, Mumbai, 400 019, India. E-mail: sv.joshi@ictmumbai.edu.in

† Electronic supplementary information (ESI) available. CCDC 2391222 and 2391223. For ESI and crystallographic data in CIF or other electronic format see DOI: **https://doi.org/10.1039/d5mr00004a**

using twin-screw extrusion (TSE) by reacting 4,4′-oxydianiline with *ortho*-vanillin under optimized conditions (120 °C, 55 rpm, feed rate: 0.79 g min^{-1}) to achieve high yields without requiring post-synthetic purification.[35] These findings establish TSE as a powerful alternative to traditional mechanochemical methods, offering enhanced scalability, improved reaction efficiency, and precise process control.

While TSE offers scalability and precise reaction control, its high cost and complexity limit accessibility.[36] To address these challenges, single-screw extrusion (SSE) has emerged as a cost-effective alternative for continuous, solvent-free organic synthesis. While SSE has been widely utilized in polymer processing, its potential in mechanochemical organic synthesis remains relatively underexplored.[37] Similar to TSE, SSE enables precise control over reaction parameters such as temperature, screw speed and residence time, but with lower operational costs and energy requirements which makes SSE an attractive option for sustainable chemical manufacturing, particularly in resource-limited settings or for processes requiring straightforward scalability.[38] In a pioneering study, Kulkarni and co-workers designed a jacketed single-screw reactor capable of operating across a temperature range of 0 °C to 160 °C and varying rotation speeds. The reactor's design features a Teflon screw housed within a condenser-type glass container, allowing for precise temperature control and visual monitoring of reactions.[39] This versatile platform facilitated various organic transformations under minimal or solvent-free conditions, thereby enhancing the efficiency and environmental friendliness of these processes.

Despite these advantages, SSE remains significantly underexplored for many organic reactions and other solvent-sensitive transformations. The lack of widespread adoption is primarily due to limited research on its mechanistic aspects, process optimization strategies and scalability beyond small laboratory-scale demonstrations. As interest in mechanochemistry keeps growing, SSE could become a practical, scalable and energy efficient alternative to traditional synthetic methods. Future studies focusing on optimizing screw design and energy input could further enhance its applicability, paving the way for SSE to be integrated into industrial-scale green synthesis.[40]

This study aims to bridge existing gaps by systematically investigating the potential of single-screw extrusion (SSE) for solvent-free imine synthesis. Optimizing temperature, screw speed and feed rate delivers near-quantitative yields without solvents or catalysts. Additionally, the versatility of SSE is explored by synthesizing imines from diverse amine substrates, including cyclic amino alcohols, amino esters and diamines, to expand the scope of this methodology. By leveraging SSE's advantages in scalability, energy efficiency and precise reaction control, this study expands the scope of mechanochemistry for continuous organic synthesis. Demonstrating its viability for high-yield, solvent-free imine production, SSE presents a transformative approach for sustainable and industrially scalable synthesis.

Results and discussion

The imine bond formation was systematically investigated using benzaldehyde and 4-*trans*-amino cyclohexanol as model substrates to address this. Initial optimization studies were conducted without the use of catalysts or a Dean–Stark apparatus, instead focusing on the influence of solvents with varying polarities. Additionally, deep eutectic solvents (DES's) were employed to assess their impact on the reaction. This method aimed to prioritize simplicity, sustainability and reproducibility, striving to establish a versatile and efficient approach that aligns seamlessly with the principles of green chemistry (Scheme 1).[41]

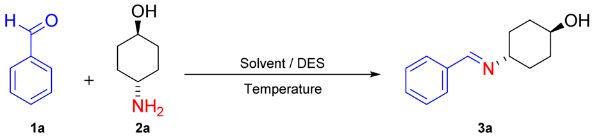

Scheme 1 A prototypical reaction of benzaldehyde **1a** with 4-*trans*-amino cyclohexanol **2a** yielding an aldimine in a batch process **3a**.

Table 1 clearly demonstrates that reactions carried out in conventional solvents under reflux conditions consistently yield moderate results (Table 1, entries 1–10). Among these, methanol provided the highest yield (Table 1, entry 2). Using aqueous solvent systems, such as water, water : methanol and water : ethanol mixtures, slightly improved the yield (Table 1, entries 11–13). This improvement is likely due to the enhanced polarity of the medium and the increased solubility of reactants, which facilitated the reaction.

To explore greener alternatives and potentially improve efficiency, deep eutectic solvents (DES's) were employed (Table 1, entries 15–19). The synthesis of choline chloride-based DES's was carried out following the procedure described in the reported methods.[42] However, these DES's did not significantly enhance the yield. The marginally improved yields in some cases could be attributed to their ability to create a hydrogen-bonded network, which might aid in stabilizing the transition state during imine formation.[43] However, in this case, the overall performance of DES's did not exceed that of traditional or aqueous systems.

Remarkably, conducting the reaction under neat conditions yielded superior results (Table 1, entries 20–22). At 80 °C, the reaction achieved a maximum yield within 30 minutes (Table 1, entry 22). Encouraged by the exceptional performance under neat conditions, further optimization studies were carried out to maximize the yield (Scheme 2).

The reaction was initially optimized under solvent-free conditions. In the initial phase, the reaction was conducted at room temperature. The conversion of aldehyde to aldimine was measured after the completion of the reaction using Gas Chromatography-Mass Spectrometry (GC-MS) analysis. Following every 10 minutes of the reaction time, thin layer chromatography (TLC) analysis was performed, which yielded no discernible results. Then, after 60 minutes of the reaction time, a trace amount of white solid formed, which was negligible to isolate. GC-MS analysis showed that benzaldehyde was left in the reaction. The molar ratio of aldehyde to amine was adjusted to 1 : 1.2, and the reaction conditions were optimized. Still, there was no improvement in the reaction, so the molar

Table 1 Yields obtained in the batch process[a]

Entry	Solvent/DES	Reaction temperature/°C	Reaction time (h)	Yield[b] (%)
1	EtOH	Reflux	3.5	31
2	MeOH	Reflux	3	34
3	Et_2O	Reflux	3.2	NR
4	EtOAc	Reflux	3	37
5	IPA	Reflux	4	25
6	DMSO	120	12	40
7	Toluene	100	4	NR[c]
8	CH_2Cl_2	Reflux	3.5	Trace
9	MeCN	Reflux	3.2	24
10	CHCl3	Reflux	2	Trace
11	H_2O	60	1.5	41
12	H_2O : EtOH (1 : 1)	60	1.5	32
13	H_2O : MeOH (1 : 1)	60	1.5	39
14	H_2O : IPA (1 : 1)	60	1.5	22
15	ChCl : urea (1 : 2)	80	2	NR[c]
16	ChCl : citric acid (1 : 1)	80	2	30
17	ChCl : citric acid (1 : 2)	100	1.5	34
18	ChCl : ethylene glycol (1 : 2)	80	1	22
19	ChCl : glycerol	80	1	Trace
20	Neat	60	0.45	44
21	Neat	70	0.30	50
22	Neat	80	0.30	54

[a] Reaction conditions: **1a** (1.0 equiv.) and **2a** (1.0 equiv.) were stirred in a 10 ml round bottom flask with the solvent (5 mL). [b] Isolated yields for **3a**. [c] No reaction.

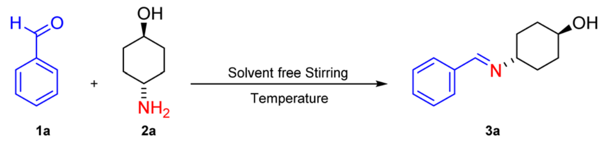

Scheme 2 Investigation of **1a** and **2a** to yield **3a** under neat conditions.

ratio was changed to 1 : 1.5. The trace amount of product yields observed at room temperatures suggests that the activation energy required for the reaction is insufficient under such conditions (Table 2, entries 1–3). In the next trial, the reaction temperature was increased to 60 °C, starting with 1 : 1.2 molar ratio, and within 30 minutes, the reaction was completed. The first trial succeeded with a significant isolated yield of the imine product (Table 2, entry 4). To evaluate the stability of the desired product in the characterization solvent, proton NMR spectra were recorded immediately after dissolution in $CDCl_3$ and monitored over time. Proton NMR analysis confirmed the formation of the imine product, as evidenced by the disappearance of the aldehyde proton and the appearance of a new imine proton at δ 8.33 ppm. Additionally, aromatic protons were observed in the range of δ 7.40–7.73 ppm, while aliphatic protons appeared at δ 1.39–3.75 ppm. The first trial resulted in a significant isolated yield of the imine product (Table 2, entry 4). No significant changes in chemical shifts, peak intensities, or the formation of additional byproducts were observed within the typical timeframe of spectral acquisition, indicating that the imine product remains stable in $CDCl_3$ under the experimental conditions (Fig. 1).

Table 2 Screening of reaction parameters in a batch process[a]

Entry	Molar ratio of reactants **1a** : **2a** (equiv.)	Reaction temperature (°C)	Time (min)	Yield[b] (%)
1	1 : 1	RT	60	Trace
2	1 : 1.2	RT	60	Trace
3	1 : 1.5	RT	60	Trace
4	1 : 1.2	60	30	51
5	1 : 1.5	60	30	52
6	1 : 1.2	90	30	60
7	1 : 1.2	100	30	64
8	1 : 1.2	110	30	69
9	1 : 1.2	120	30	43

[a] Reaction conditions: solvent free stirring of **1a** and **2a** in a 10 ml round bottom flask and heated using an oil bath. [b] Isolated yields for **3a**.

Optimization began by considering reaction parameters such as temperature, time and the molar ratio of amine. From the previous trial, it was observed that imine formation appeared at the reaction temperature of 60 °C; this time, the molar ratio was increased to 1 : 1.5, keeping the temperature constant to observe any changes in the reaction. However, there was no major change in the yield of the product. Therefore, the molar ratio was reduced to 1 : 1.2, and the reaction temperature was raised. To standardize the reaction time and obtain the maximum yield, 30 minutes of reaction time was chosen, with reaction monitoring every 10 minutes to ensure complete conversion of the aldehyde to aldimine. The reaction temperature was set to 90 °C, aiming for a better yield than the previous

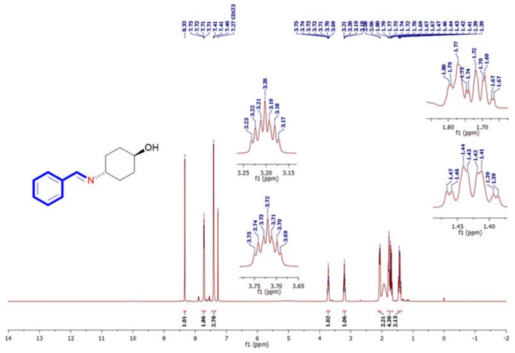

Fig. 1 ^{1}H-NMR of crude product **3a** in $CDCl_3$.

Table 3 Mechanochemical approach to cyclohexanol imines using a mortar and pestle grinding method[a]

Entry	R_1	Time (min)	Yield[b] (%)
1	**1a**, H	25	**3a**, 72
2	**1b**, 2F	20	**3b**, 75
3	**1c**, 4F	20	**3c**, 68
4	**1d**, 4CN	18	**3d**, 77
5	**1e**, OMe	30	**3e**, 54

[a] Reaction conditions: reactions were carried out using neat grinding, **1a–e** (1.0 equiv.) and **2a** (1.2 equiv.) at room temperature. [b] Isolated yields.

batch. Surprisingly, within 10 minutes, a new spot appeared, although the starting material was still present in the reaction. This indicates that temperature is a key factor for this reaction. An isolated yield comparable to previous experiments was achieved (Table 2, entry 6). This study showed that an increase above room temperature was sufficient to facilitate this reaction concerning reaction time. The optimization studies progressed with a systematic increase in reaction temperature, ultimately reaching 120 °C. It was observed that the efficiency of the reaction improved significantly at a certain temperature, highlighting it as the most favourable condition for the process (Table 2, entry 8). However, it is important to note that a further increase in temperature led to a marked decrease in yield, likely due to thermal degradation of the aldimine product, as indicated by the significant drop at 120 °C (Table 2, entry 9).

Given the results achieved under neat conditions, the impact of grinding with a mortar and pestle, which utilizes the mechanical energy generated to drive chemical transformations, was further explored.[44] To assess the feasibility and efficacy of this approach, four different benzaldehyde substrates, including benzaldehyde **1a**, were chosen for grinding under solvent-free conditions using a mortar and pestle. The reaction was optimized by maintaining a 1 : 1.2 molar ratio of aldehyde to amine, ensuring effective mixing and maximising the yield at room temperature (Scheme 3).

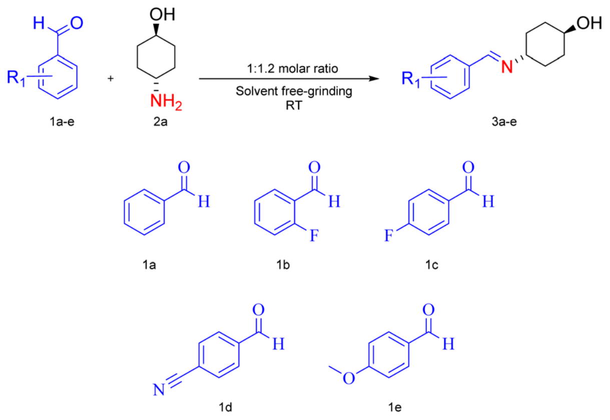

Scheme 3 Scope of the synthesis of cyclohexanol aldimine using the grinding method.

Benzaldehyde (**1a**) worked well, completing the reaction in 25 minutes and producing a good yield (Table 3, entry 1). In contrast, 2-fluorobenzaldehyde (**1b**) reacted in a shorter time of 20 minutes while producing a yield marginally higher than that of (**1a**) (Table 3, entry 2). It is believed that the fluorine atom at the *ortho* position enhances the electrophilicity of the carbonyl group through its moderate electron-withdrawing effect, facilitating nucleophilic attack by the amine group. Similarly, 4-fluorobenzaldehyde (**1c**) completed the reaction within 20 minutes, producing a yield slightly lower than that of **1b**. This difference can be attributed to the *para* position of the fluorine atom, which exerts a less pronounced inductive effect compared to the *ortho* position, affecting the electrophilic nature of the aldehyde (Table 3, entry 3).

The highest yield was observed with 4-cyanobenzaldehyde (**1d**) (Table 3, entry 4), which completed the reaction in less than 20 minutes. The strong electron-withdrawing nature of the cyano group significantly increases the aldehyde's electrophilicity, thereby accelerating imine bond formation. Conversely, 4-methoxybenzaldehyde (**1e**), due to its electron-donating methoxy group, displayed the slowest reaction time which took 30 minutes and yielded less product as compared to the other substrates. This behaviour can be attributed to the resonance-donating effect of the methoxy group, which decreases the electrophilic nature of the aldehyde, making it less reactive in the condensation process (Table 3, entry 5). This reduction in reactivity can be explained by the electron-donating resonance effect, which reduces the electrophilic character of the aldehyde group.[45]

The grinding method demonstrated satisfactory results (Table 3) for small-scale mechanochemical synthesis with cyclohexanol aldimines; however, it is essential to address the challenges related to scalability and yield optimization. As a result, mechanochemical synthesis using a single-screw hot melt extruder was chosen, as it allows for fine-tuning of temperature and residence time, which are critical for driving product formation to completion. The continuous mixing provided by the extruder also ensures that the reactants remain in close contact, enhancing reaction efficiency and promoting uniform heat distribution (Scheme 4).[46]

The mechanochemical synthesis of **3a** *via* single-screw hot melt extrusion was systematically investigated at varying temperatures (32–140 °C) and screw speeds (45–90 rpm). Key

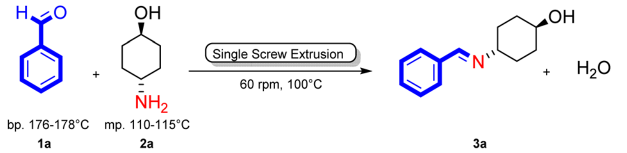

Scheme 4 Synthesis of a cyclohexanol aldimine in a single screw hot melt extruder.

parameters such as residence time, feed rate, product throughput and space time yield (STY) were quantified to evaluate the process efficiency (Table 4). The extruder's modular design comprising feed, conveying, mixing and metering zone enabled precise control over reaction conditions, aligning with advancements in continuous mechanochemical synthesis.[47] The first trial was conducted at room temperature with a screw speed of 90 rpm, where the mixture of **2a** (56.5 mmol, 6.51 g) and **1a** (47 mmol, 5 g) was manually fed into the extruder over a 7-minute period through the feeding zone (feed rate 1.644 g min^{-1}, residence time: 6 min); anticipating that the frictional heat generated by the screw speed would initiate the reaction. However, minimal product formation (2.48 g, 26% yield) was observed, indicating that the frictional heat generated by mechanical shearing alone was insufficient to drive the reaction to completion (Table 4, entry 1). This finding is consistent with prior studies emphasizing the necessity of supplemental thermal energy in mechanochemical reactions involving low-melting-point substrates.[22] Increasing the barrel temperature to 60 °C significantly improved the product yield (3.82 g, 40% yield) while maintaining a residence time of 6 minutes and a feed rate of 1.92 g min^{-1} (Table 4, entry 2). Further elevation to 90 °C enhanced conversion efficiency, reducing the residence time to 5 minutes (feed rate: 2.30 g min^{-1}) and yielding 8.50 g (89% yield) of the desired product (Table 4, entry 3). The highest yield of 97% was obtained at 100 °C, where the residence time was about 3–4 minutes with a feed rate of 3.29 g min^{-1}, suggesting that this temperature provided the optimal activation energy for imine formation (Table 4, entry 4). This temperature provided the optimal activation energy for imine formation without causing product degradation, despite being significantly lower than the melting points of **2a** (110–115 °C) and **1a** (176–178 °C). However, a sudden decrease in yield was observed due to the formation of a semisolid mixture when the temperature was increased to 110 °C (Table 4, entry 5) which is likely attributable to thermal degradation of the product. The corresponding space-time yield, *i.e.*, the amount of product mass per unit extruder volume (STY) further supports these findings, with the highest STY of 644.34 kg m^{-3} day^{-1} achieved at 100 °C (Table 4, entry 4). This value demonstrates the efficiency of the extruder in achieving high throughput under optimized conditions without any further post-purification {note: the reaction mass was carefully handled during sampling. Before each analysis, the reaction mass was allowed to cool and then washed thoroughly with cold distilled water. The washed and dried reaction mass was subsequently subjected to monitoring}.

Thermal studies by differential scanning calorimetry (DSC)

The DSC thermograms of compound **3a** revealed some differences in crystallinity and thermal behavior based on the synthesis methods, providing insight into the influence of preparation techniques on sample properties (Fig. 2).

The thermogram for **3a′S1**, synthesized *via* the single screw extrusion (SSE) method, displayed a sharp endothermic peak at approximately 92 °C (Fig. 2A). This indicates a high degree of crystallinity and suggests that the SSE method effectively promotes uniform mixing and controlled synthesis conditions, which in turn enhances the thermal stability of the compound.

On the other hand, the thermogram for **3aa′-S2**, prepared using the mortar and pestle grinding method, exhibited a sharp endothermic peak at 92.2 °C, but with an additional, broader thermal feature between 100 and 120 °C (Fig. 2B). The presence of this broader thermal region points to structural heterogeneity, possibly due to minor impurities, amorphous regions or secondary thermal events.[48,49] This suggests that the grinding method, although effective to an extent, may not provide the same level of uniformity and structural precision as the SSE method.

These observations show that the extrusion method produces more stable and crystalline compounds, offering superior control over the synthesis process. The marked difference in the thermal profiles between the two methods highlights the critical role of preparation techniques in shaping the thermal properties and crystallinity of the materials. Overall, the SSE method stands out as an optimal choice for thermally stable and uniform products, particularly in solvent-free mechanochemical processes.[50]

With the optimized conditions established for the aldimine synthesis of **3a** using single-screw hot melt extrusion, the scope

Table 4 Optimization of single screw extruder parameters in the extrusion[a] of **2a** with **1a**

Entry	Temperature (°C)	Residence time (min)	Feed rate (g min^{-1})	Product throughput (g min^{-1})	Space-time yield (kg m^{-3} day^{-1})
1	32	6.0	1.64	0.413	100.80
2	60	6.0	2.30	0.636	155.23
3	90	5.0	2.88	1.70	414.92
4	100	3.5	2.30	2.64	644.34
5	110	4.0	2.30	1.935	472.27

[a] Reaction conditions: **2a** (56.5 mmol, 6.51 g) (1.2 equiv.), **1a** (47 mmol, 5 g) (1.0 equiv.), single screw extruder, screw speed: 90 rpm, temperature as specified.

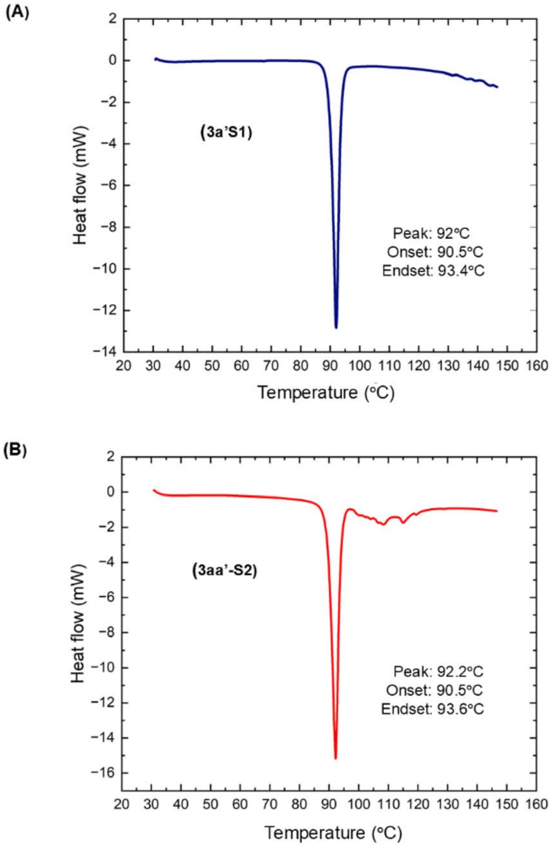

Fig. 2 (A and B) DSC thermograms of **3a** from the extrusion and grinding methods, respectively.

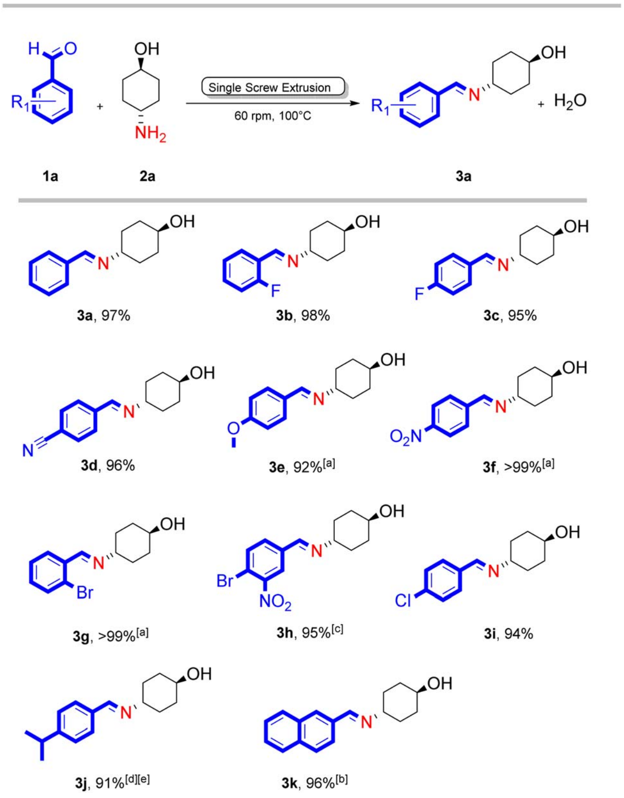

Scheme 5 Scope of cyclohexanol imine synthesis using SSE. Reaction conditions: aldehyde **1** (5 g, 1.0 equiv.), *trans*-4-aminocyclohexanol **2a** (1.2 equiv.), single screw extruder, 90 rpm, 100 °C. Yields reported are isolated yields. [a] Extrusion temperature: 110 °C, [b] 120 °C, [c] 130 °C, [d] 140 °C. [e] 1.5 equiv. amine.

of the reaction was extended to benzaldehyde derivatives bearing electron-withdrawing as well as electron-donating substituents (Scheme 5). A slight excess of amine (extra 0.2 equiv.) was used in each case to achieve favourable yields. Notably, substrates with electron-withdrawing groups exhibited enhanced reactivity, whereas those with electron-donating groups showed slightly reduced efficiency. As shown in Scheme 5, aldimines derived from *ortho*- and *para*-substituted electron-withdrawing groups (**3b–3d**) exhibited excellent yields with a shorter residence time (Table 5). Temperature played a crucial role in reaction outcomes. For instance, **3e**, which provided 89% yield at 100 °C (residence time 4 min), showed improved efficiency at 110 °C, reaching 92% with a reduced residence time of 3 minutes. Similarly, compound **3f** exhibited a 95% yield at 100 °C, which increased to near-quantitative conversion (>99%) at 110 °C with a residence time of 3 min. This trend continued with **3g**, where incremental temperature increases further enhanced product formation (see Fig. 3 for the ORTEP diagram of **3g**). Conversely, **3h** required a higher barrel temperature of 130 °C to attain optimal yields, despite an initial moderate yield of 92% at 100 °C. Bulky and sterically hindered substrates, such as **3j**, benefited from increased barrel temperature and an excess of amine (extra 0.5 equiv.), with yields increasing from 85% at 100 °C to 91% at 140 °C. Likewise, **3k** showed enhanced reactivity at elevated temperatures, increasing from 91% at 100 °C to 96% at 120 °C (Scheme 5).

Encouraged by the successful synthesis of aldimines from cyclohexanol amines, the investigation was extended to a more challenging amine substrate L-phenylalaninate methyl ester, a liquid amine synthesized from L-phenylalanine (Scheme 6).[51]

Building on the successful aldimine synthesis using **2a**, the reaction scope was expanded to include methyl L-phenylalaninate (**2b**), a liquid amino ester derivative of L-phenylalanine. Initial attempts to perform the reaction as a liquid–liquid system revealed significant challenges. Upon premixing the two liquid reactants 4-methylbenzaldehyde and **2b**, a solid formation was observed. This led to the formation of lumps, which hindered mixing and resulted in inhomogeneous reaction conditions. The solidification also made it difficult to maintain a consistent flow of reactants, further complicating the process. To address these issues, the reaction was attempted in the extruder using a syringe pump to feed the liquid reactants. However, this approach also proved problematic. Despite the controlled feeding of reactants, poor mixing and inefficient reaction conditions were observed, leading to suboptimal yields. To overcome this challenge, sodium chloride (NaCl) was introduced as a solid additive. NaCl acted as a process aid, improving the flow properties of the reaction mixture and

Table 5 Process parameters for cyclohexanol imine synthesis *via* single screw extrusion[a]

Product	Temperature (°C)	Residence time (min)	Feed rate (g min^{-1})	Product throughput (g min^{-1})	Space time yield (kg m^{-3} day^{-1})
3a	100	3.5	2.30	2.64	644.34
3b	100	3	1.76	2.91	710.64
3c	100	4	1.76	2.12	517.63
3d	100	4.5	2.05	1.86	453.56
3e	110	3.3	1.68	2.39	583.64
3f	110	3	1.91	2.72	664.68
3g	110	3–3.5	1.09	2.53	528.82
3h	130	5	1.60	1.35	329.49
3i	100	3.5	1.98	2.27	554.24
3j	140	5	0.97	1.51	368.14
3k	120	2.5–3	1.18	3.11	633.22

[a] For each extrusion the screw speed was 90 rpm. Further discussion is presented in the ESI.

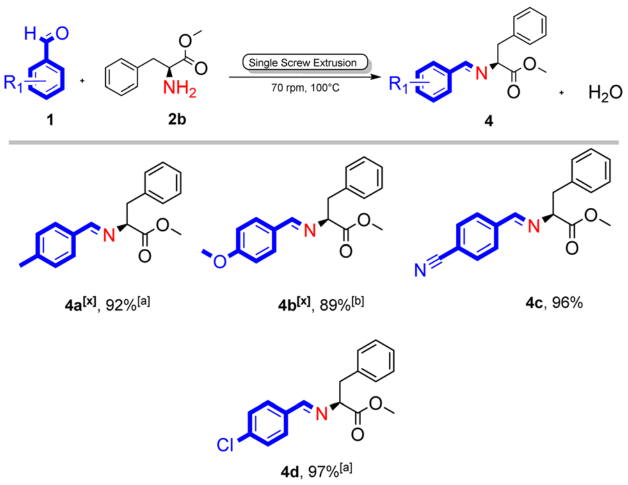

Scheme 6 Scope of phenylalaninate imine synthesis using SSE. Reaction conditions: aldehyde **1** (5 g, 1.0 equiv.), methyl L-phenylalaninate **2b** (1.2 equiv.), single screw extruder, 70 rpm, 100 °C. Yields reported are isolated yields. [x] 10 g NaCl was premixed with amine. [a] Extrusion temperature: 110 °C, [b] 120 °C.

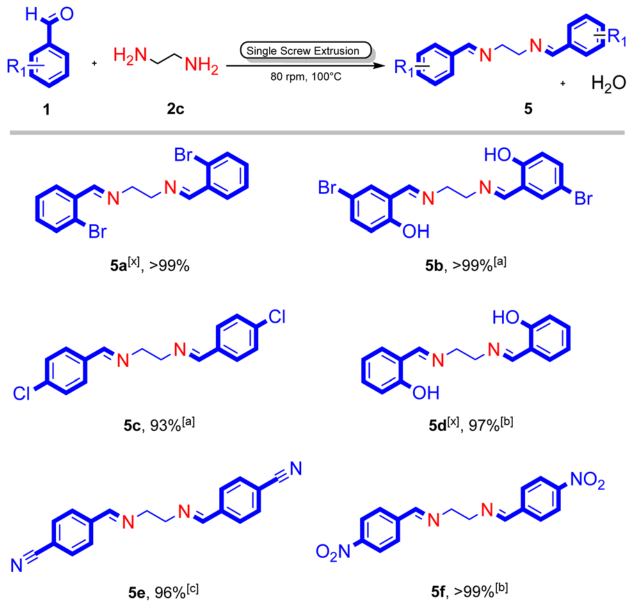

Scheme 7 Scope of di-imine synthesis using SSE. Reaction conditions: ethylene diamine **2g** (2 g, 1.0 equiv.), aldehyde 1 (2.0 equiv.), single screw extruder, 80 rpm, 100 °C. Yields reported are isolated yields. [x] 5 g NaCl was premixed with amine. [a] Extrusion temperature: 110 °C, [b] 120 °C.

preventing the formation of lumps. The amine (**2b**) was premixed with NaCl to ensure homogeneous distribution before being combined with 4-methylbenzaldehyde. This mixture was then fed into the extruder, at a screw speed of 70 rpm where the presence of NaCl facilitated smoother flow and better mixing, even as the reaction proceeded to form the solid product (feed rate: 1.99 g min^{-1}) (Scheme 7).

The reaction of 4-methylbenzaldehyde and **2b** at 100 °C afforded the desired product **4a** with an isolated yield of 90% and a residence time of 5 minutes. Elevating the barrel temperature to 110 °C further optimized the process, with an isolated yield of 92% and a space-time yield (STY) of 525.36 kg m^{-3} day^{-1} (see Fig. 4 for the ORTEP diagram of **4a**). In contrast, synthesizing **4b** proved more challenging. Consistent with previous reactions, sodium chloride (NaCl) was employed as an additive to facilitate the process. At a barrel temperature of 100 °C, the reaction yielded 86%, while increasing the temperature to 110 °C improved the yield to 87%. Further optimization at 120 °C resulted in a yield of 89%. Notably, **4c** and **4d** exhibited excellent reactivity. For **4c,** a barrel temperature of 100 °C was sufficient to achieve a high yield of 96% with a residence time of 4 minutes and a feed rate of 2.64 g min^{-1}. In the case of **4d,** a barrel temperature of 100 °C afforded a yield of 93% (residence time: 4 minutes), while increasing the temperature to 110 °C further enhanced the yield to 97% with a reduced residence time of 3 minutes. The improved reactivity of **4d** at elevated temperatures is consistent with the enhanced electrophilicity imparted by the electron-withdrawing substituents (Table 6).

The scope of extrusion-based imine synthesis was expanded to include the preparation of di-imines using single-screw extrusion (SSE) at a screw speed of 80 rpm. Ethylene diamine

Table 6 Process parameters for phenylalaninate imine synthesis *via* single screw extrusion[a]

Product	Temperature (°C)	Residence time (min)	Feed rate (g min^{-1})	Product throughput (g min^{-1})	Space time yield (kg m^{-3} day^{-1})
4a	110	5	1.99	2.15	525.36
4b	120	3	2.15	3.24	791.19
4c	100	4	2.64	2.66	652.88
4d	110	3	2.53	2.60	848.14

[a] For each extrusion the screw speed was 70 rpm. Further discussion is presented in the ESI.

Table 7 Process parameters for di-imine synthesis *via* single screw extrusion[a]

Product	Temperature (°C)	Residence time (min)	Feed rate (g min^{-1})	Product throughput (g min^{-1})	Space time yield (kg m^{-3} day^{-1})
5a	100	3	2.86	4.33	1059.32
5b	110	2	3.08	4.68	1716.61
5c	110	3.5	1.34	2.69	656.68
5d	120	3	1.69	2.88	705.76
5e	140	3	2.14	3.04	745.42
5f	120	3	2.41	2.56	874.58

[a] For each extrusion the screw speed was 80 rpm. Further discussion is presented in the ESI.

(**2c**) served as the amine substrate under optimized reaction conditions. Yields exceeding 99% were achieved in most cases, with residence times ranging from 2 to 4 minutes. For the synthesis of **5a**, ethylene diamine (33.27 mmol, 1.0 equiv.) adsorbed with NaCl and 2-bromobenzaldehyde (66.55 mmol, 2.0 equiv.) were manually fed into the extruder over 5 minutes (feed rate: 2.86 g min^{-1}, residence time: 3 minutes), which afforded the desired di-imine product with an isolated yield of >99% which had a throughput rate of 4.33 g min^{-1} which is 6.24 kg day^{-1}. A slight drop in yield was observed for **5a** when the barrel temperature was increased from 100 °C to 110 °C. In the case of **5b**, a barrel temperature of 100 °C provided an isolated yield of 94% (residence time: 3 minutes), while increasing the temperature to 110 °C improved the yield to >99% (residence time: 2 minutes). Under the current extrusion conditions, a potential throughput of 6.74 kg day^{-1} could be achieved, suggesting the feasibility of scaling up this process to industrial levels. Products **5c–5e** exhibited yields of 93–97% at barrel temperatures between 100 °C and 140 °C, with shorter residence times of 3–4 minutes. The synthesis of **5f** required careful optimization of reaction conditions. At 100 °C, the isolated yield was 95% (residence time: 5 minutes, feed rate: 2.41 g min^{-1}). Increasing the temperature to 110 °C enhanced the yield to 96% (residence time: 4 minutes), and further elevation to 120 °C resulted in a yield of >99% (residence time: 3 minutes). Overall, the efficiency of di-imine synthesis was influenced by the

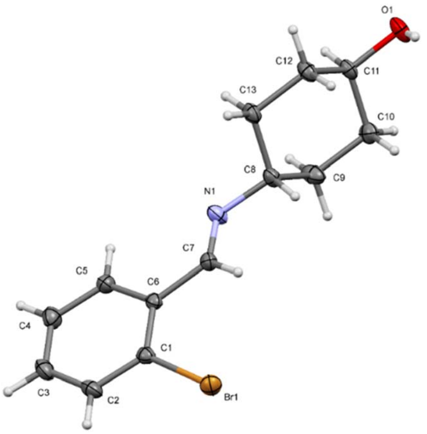

Fig. 3 ORTEP diagram for compound **3g**. Displacement ellipsoids are drawn at the 30% probability level and H atoms are shown as small spheres of arbitrary radius.

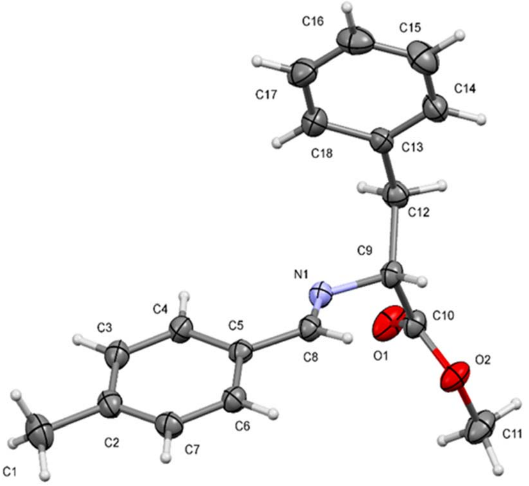

Fig. 4 ORTEP drawing for **4a**. Displacement ellipsoids are drawn at the 30% probability level and H atoms are shown as small spheres of arbitrary radius.

functional groups attached to the substrates, with electron-withdrawing groups demonstrating enhanced reactivity and yields (Table 7).

Conclusion

This study successfully demonstrated the one-pot synthesis of aldimines *via* single-screw extrusion (SSE), offering a sustainable, solvent-free mechanochemical approach. By optimizing key parameters such as temperature, screw speed, and feed rate, the method achieved high to near-quantitative yields (>99% for selected derivatives) across diverse substrates, including cyclohexanol amines, L-phenylalaninate methyl esters and ethylenediamine-derived bis-aldimines. The SSE process outperformed traditional batch methods and mechanochemical grinding in terms of efficiency and crystallinity as evidenced by sharper DSC endothermic peaks and scalability, with a remarkable throughput rate of 6.74 kg day^{-1} and a space-time yield of 1716 kg m^{-3} day^{-1}. The versatility of SSE was highlighted by its ability to accommodate substrates with both electron-withdrawing and electron-donating groups, with the former exhibiting enhanced reactivity. Challenges such as inhomogeneous mixing in liquid–liquid systems were addressed using solid additives like NaCl, further underscoring the adaptability of SSE.

In conclusion, SSE represents a scalable, efficient and environmentally friendly alternative to conventional imine synthesis methods. Its potential extends beyond aldimines, offering a platform for diverse mechanochemical transformations in pharmaceutical and materials science applications. Future work could explore screw design modifications and broader substrate scopes to further enhance its industrial applicability.

Perspectives

While this study establishes single-screw extrusion (SSE) as an efficient platform for solvent-free aldimine synthesis, several promising research directions emerge from our findings. First, the demonstrated role of the NaCl additive in enhancing liquid amine reactivity suggests new opportunities for developing optimized solid-phase catalysts or ionic additives to further improve reaction selectivity and efficiency.

A systematic study by Lu *et al.* on the role of acids and hydrogen bond acceptors in enamine equilibria highlights how additives can profoundly influence reaction pathways.[52] This insight is particularly relevant for our mechanochemical system, where competing reaction pathways remain to be fully elucidated. Systematic investigation of these pathways under SSE conditions could provide a fundamental understanding of mechanochemical enamine equilibria. Furthermore, expanding the substrate scope to include sterically hindered amines and bifunctional substrates may unlock novel applications in pharmaceutical synthesis and functional materials development. We are currently pursuing these directions through carefully designed experimental studies.

Data availability

Crystallographic data for the structures reported in this work have been deposited with the Cambridge Crystallographic Data Centre (CCDC) under deposition numbers 2391222 and 2391223. Copies of these data can be obtained free of charge *via* www.ccdc.cam.ac.uk/data_request/cif. All supporting experimental data, including detailed synthetic procedures, full spectroscopic characterization and DSC thermograms are available in the ESI.†

Author contributions

ASL conceived the study, designed and performed the SSE experiments, conducted analytical characterization and led the manuscript writing. KVS validated the data analysis and curated the experimental data along with performing experiments and conducting analysis along with ASL. SSP managed resources and handled project administration. SVJ supervised the project, secured funding and oversaw resource allocation. All authors have read and approved the submitted manuscript.

Conflicts of interest

There are no conflicts to declare.

Acknowledgements

The authors sincerely thank Prof. Aniruddha B. Pandit, Vice Chancellor, and the Departments of Pharmaceutical Sciences and Technology and Chemistry at the Institute of Chemical Technology, Mumbai, for their infrastructure support. This research was conducted without external funding.

Notes and references

1 P. Xiao, N. Chen, J. Liu, L. Yang, D. Chen and M. Shi, *Prog. Org. Coat.*, 2024, **186**, 108017.

2 G. A. Aleku, *ACS Catal.*, 2024, **14**, 14308–14329.

3 R. Li, Y. Yang, Z. Zhang, S. Lian and C. Song, *J. Membr. Sci.*, 2024, **690**, 122203.

4 M. Abdullahi, A. Uzairu, G. A. Shallangwa, P. A. Mamza, M. T. Ibrahim, A. Chandra and V. K. Goel, *J. Biomol. Struct. Dyn.*, 2024, **42**, 2013–2033.

5 G. Singh, Heena, B. S. Gill, D. Baliyan, S. Gupta, S. C. Sahoo, Vikas, C. Espinosa-Ruíz and M. A. Esteban, *J. Mol. Liq.*, 2024, **412**, 125867.

6 Y. Pan, Z. Li, S. Shen, D. Liu and G. Zhang, *Colloids Surf., A*, 2024, **686**, 133431.

7 H. Kargar, M. Fallah-Mehrjardi, M. Moghadam, S. Yarahmadi, A. Omidvar, H. R. Zare-Mehrjardi, N. Dege, M. Ashfaq, K. S. Munawar, M. N. Tahir and H. R. Shahsavari, *Inorg. Chim. Acta*, 2024, **570**, 122160.

8 H. Chen, Z. Liu, Y. Xu, X. Yu, Y. Tao, Y. Li, X. Huang, J. He and T. Wang, *Chem. Sci.*, 2025, **16**, 4295–4302.

9 (*a*) X. Hu, A. M. Jazani and J. K. Oh, *Polymer*, 2021, **230**, 124024; (*b*) J. Anane, E. Owusu, G. Rivera and

D. Bandyopadhyay, *IJMS*, 2024, **25**, 2263; (*c*) J.-S. Tian, Z. Tu, F. Zhou, J.-S. Yu and J. Zhou, *Org. Chem. Front.*, 2023, **10**, 1759–1766.

10 (*a*) K. Li, S. Wang, Y. Jiang, M. Chen, W. Dong and D. Shi, *J. Appl. Polym. Sci.*, 2025, e57033; (*b*) P. Stiernet and A. Debuigne, *Prog. Polym. Sci.*, 2022, **128**, 101528; (*c*) S. K. Schoustra, T. Groeneveld and M. M. J. Smulders, *Polym. Chem.*, 2021, **12**, 1635–1642.

11 (*a*) Y. Wen, L. Yuan, R. Li, S. Chen, B. Tang, X. Tang, W. Zhang, S. Cai and J. Fan, *Colloids Surf., A*, 2024, **688**, 133661; (*b*) J.-F. Li, J.-W. Xu, H.-J. Feng, Q.-Y. Liu and J.-W. Wang, *New J. Chem.*, 2025, **49**, 6838–6845.

12 (*a*) A. K. Saini, P. Kumari, V. Sharma, P. Mathur and S. M. Mobin, *Dalton Trans.*, 2016, **45**, 19096–19108; (*b*) W. Al Zoubi, S. G. Mohamed, A. A. S. Al-Hamdani, A. P. Mahendradhany and Y. G. Ko, *RSC Adv.*, 2018, **8**, 23294–23318; (*c*) J. Koh, C. A. Baker, M. N. Diamantakis, N. J. Long and C. Romain, *Polym. Chem.*, 2025, **16**, 1503–1508; (*d*) J. E. L. Payong, N. G. Léonard, L. M. Anderson-Sanchez, J. W. Ziller and J. Y. Yang, *Dalton Trans.*, 2025, **54**, 934–941; (*e*) Y.-F. Liu, G. Gil-Ramírez and T. Nakamura, *Chem. Commun.*, 2025, **61**, 921–924; (*f*) A. Mishra, J. Hu, X. Cong, Q. Zhuo, M. Nishiura, G. Luo and Z. Hou, *Angew. Chem.*, 2025, **137**, e202419567.

13 (*a*) N. Ganji, B. Karimi and H. Vali, *ACS Appl. Nano Mater.*, 2024, **7**, 2650–2661; (*b*) M. S. S. Adam, A. Taha, A. T. Hereba, M. M. Makhlouf and H. A. Mahmoud, *Appl. Organomet. Chem.*, 2024, **38**, e7438; (*c*) J. Mohapatra, S. Nath, M. Sahu, S. Ghosh, A. Puthukkudi, M. Saifuddin, S. Bommakanti, C. V. Rajput, M. Samal, S. P. Senanayak and B. P. Biswal, *Chem. Mater.*, 2024, **36**, 1536–1546.

14 (*a*) R. D. Patil and S. Adimurthy, *Asian J. Org. Chem.*, 2013, **2**, 726–744; (*b*) S. Morales, F. G. Guijarro, J. L. García Ruano and M. B. Cid, *J. Am. Chem. Soc.*, 2014, **136**, 1082–1089; (*c*) J.-M. Huang, J.-F. Zhang, Y. Dong and W. Gong, *J. Org. Chem.*, 2011, **76**, 3511–3514; (*d*) A. Zanardi, J. A. Mata and E. Peris, *Chem.–Eur. J*, 2010, **16**, 10502–10506; (*e*) D. D. Mal and D. Pradhan, *Inorg. Chem.*, 2022, **61**, 2211–2218.

15 (*a*) K. Ciesielska, M. Hoffmann, M. Kubicki and D. Pluskota-Karwatka, *Molecules*, 2022, **27**, 4557; (*b*) B. R. Naidu, T. Sruthi, R. Mitty and K. Venkateswarlu, *Green Chem.*, 2023, **25**, 6120–6148; (*c*) M. Banerjee, P. C. Panjikar, D. Das, S. Iyer, A. A. Bhosle and A. Chatterjee, *Tetrahedron*, 2022, **112**, 132753.

16 (*a*) P. Mayavel, J. Divya, P. Gayathri, S. Balasundari, V. Usha, I. Muthuvel, K. Balu, K. N. Shivakumara, G. Raman and G. Thirunarayanan, *Res. Chem. Intermed.*, 2024, **50**, 4503–4532; (*b*) X. Chen, S. Li, S. Sun and W. Sun, *React. Chem. Eng.*, 2025, **10**, 22–26; (*c*) W. Zhao, P. Yan, H. Yang, M. Bahri, A. M. James, H. Chen, L. Liu, B. Li, Z. Pang, R. Clowes, N. D. Browning, J. W. Ward, Y. Wu and A. I. Cooper, *Nat. Synth.*, 2022, **1**, 87–95.

17 (*a*) V. T. Lee, J. Kellenberger, K. Borton and S. D. Montag, *J. Chem. Educ.*, 2024, **101**, 5129–5133; (*b*) M. Nigam, D. Tuttle, B. Morra, A. P. Dicks and J. Rodriguez, *Green Chem. Lett. Rev.*, 2023, **16**, 2185107; (*c*) J. Fu, Y. Yue, K. Liu, S. Wang, Y. Zhang, Q. Su, Q. Gu, F. Lin and Y. Zhang, *Mol. Diversity*, 2023, **27**, 873–887.

18 (*a*) S. Kauser, Q. Ullah, M. Arifuddin, S. Ahmad Khan and A. Rehman, *Results Chem.*, 2023, **5**, 100839; (*b*) N. Kawahara, K. Palasin and Y. Asano, *Catalysts*, 2022, **12**, 511.

19 (*a*) J. C. Lopes, T. Moniz, M. J. Sampaio, C. G. Silva, M. Rangel and J. L. Faria, *Catal. Today*, 2023, **418**, 114045; (*b*) H. Xu, J.-L. Shi, H. Hao, X. Li and X. Lang, *Catal. Today*, 2019, **335**, 128–135; (*c*) X.-J. Li, H.-T. Wan, M.-Y. Qi, C.-L. Tan and Z.-R. Tang, *Mol. Catal.*, 2024, **564**, 114356.

20 L. H. Park, E. M. Leitao and C. C. Weber, *Org. Biomol. Chem.*, 2024, **22**, 202–227.

21 (*a*) J. Batteas, K. G. Blank, E. Colacino, F. Emmerling, T. Friščić, J. Mack, J. Moore, M. E. Rivas and W. Tysoe, *RSC Mechanochem.*, 2025, **2**, 10–19; (*b*) J. Alić, M. Schlegel, F. Emmerling and T. Stolar, *Angew. Chem., Int. Ed.*, 2024, **63**, e202414745.

22 (*a*) F. Basoccu, L. De Luca and A. Porcheddu, *Eur. J. Org Chem.*, 2024, **27**, e202400425; (*b*) R. S. Atapalkar and A. A. Kulkarni, *React. Chem. Eng.*, 2024, **9**, 10–25; (*c*) N. Fantozzi, J.-N. Volle, A. Porcheddu, D. Virieux, F. García and E. Colacino, *Chem. Soc. Rev.*, 2023, **52**, 6680–6714.

23 (*a*) S. Pagola, *Crystals*, 2023, **13**, 124; (*b*) M. Baláž, V. Balema, J. D. Batteas, R. G. Blair, C. Bolm, L. Borchardt, A. B. Braunschweig, S. L. Craig, F. Emmerling, M. Ferguson, T. Friščić, S. James, J. Leitch, J. Mack, S. Mohamed, K. Nagapudi, F. Puccetti and M. E. Rivas, *Faraday Discuss.*, 2023, **241**, 387–393.

24 P. Baláž, M. Achimovičová, M. Baláž, P. Billik, Z. Cherkezova-Zheleva, J. M. Criado, F. Delogu, E. Dutková, E. Gaffet, F. J. Gotor, R. Kumar, I. Mitov, T. Rojac, M. Senna, A. Streletskii and K. Wieczorek-Ciurowa, *Chem. Soc. Rev.*, 2013, **42**, 7571.

25 V. Martinez, T. Stolar, B. Karadeniz, I. Brekalo and K. Užarević, *Nat. Rev. Chem*, 2022, **7**, 51–65.

26 J. Joy, A. Krishnamoorthy, A. Tanna, V. Kamathe, R. Nagar and S. Srinivasan, *Appl. Sci.*, 2022, **12**, 9312.

27 (*a*) L. Buglioni, F. Raymenants, A. Slattery, S. D. A. Zondag and T. Noël, *Chem. Rev.*, 2022, **122**, 2752–2906; (*b*) A. Krusenbaum, S. Grätz, G. T. Tigineh, L. Borchardt and J. G. Kim, *Chem. Soc. Rev.*, 2022, **51**, 2873–2905.

28 (*a*) A. Gallos, G. Paës, F. Allais and J. Beaugrand, *RSC Adv.*, 2017, **7**, 34638–34654; (*b*) N. Thyashan, Y. S. Perera, R. Xiao and C. Abeykoon, *Int. J. Lightweight Mater. Manuf.*, 2024, **7**, 353–361.

29 (*a*) H. Morrison, P. Fung, T. Tran, E. Horstman, E. Carra and S. Touba, *Org. Process Res. Dev.*, 2018, **22**, 1432–1440; (*b*) H. Morrison, P. Fung, E. Horstman, O. Lapina, T. Khuth, D. S. Lye, C. S. Regens, D. Bringley and J. Alleva, *Org. Process Res. Dev.*, 2024, **28**, 1186–1194; (*c*) M. Lavayssiere and F. Lamaty, *Chem. Commun.*, 2023, **59**, 3439–3442.

30 (*a*) Sabirin, A. B. Sitanggang, S. Budijanto, M. B. Kusarpoko, A. Darussalam, A. S. Purwoto and Y. S. Pramana, *Food Measure*, 2024, **18**, 3793–3805; (*b*) R. J. Kowalski, E. Pietrysiak and G. M. Ganjyal, *J. Food Eng.*, 2021, **303**, 110589; (*c*) L. G. Trujillo-Juárez, Ó. Hernández-Meléndez,

M. Gimeno, J. Gracia-Fadrique and E. Bárzana, *ACS Food Sci. Technol.*, 2021, **1**, 1198–1205.

31 (*a*) R. R. A. Bolt, J. A. Leitch, A. C. Jones, W. I. Nicholson and D. L. Browne, *Chem. Soc. Rev.*, 2022, **51**, 4243–4260; (*b*) Q. Cao, D. E. Crawford, C. Shi and S. L. James, *Angew. Chem., Int. Ed.*, 2020, **59**, 4478–4483; (*c*) R. Milotskyi, G. Sharma, T. Fujie, D. Hirose, N. Wada and K. Takahashi, *React. Chem. Eng.*, 2023, **8**, 1395–1402; (*d*) D. E. Crawford, A. Porcheddu, A. S. McCalmont, F. Delogu, S. L. James and E. Colacino, *ACS Sustainable Chem. Eng.*, 2020, **8**, 12230–12238; (*e*) D. E. Crawford, S. L. James and T. McNally, *ACS Sustainable Chem. Eng.*, 2018, **6**, 193–201.

32 (*a*) D. Daurio, K. Nagapudi, L. Li, P. Quan and F.-A. Nunez, *Faraday Discuss.*, 2014, **170**, 235–249; (*b*) J. M. Vasoya, H. L. Lee, T. Lee and A. T. M. Serajuddin, *Mol. Pharmaceutics*, 2023, **20**, 5160–5172.

33 (*a*) Y. Quan, R. Shen, R. Ma, Z. Zhang and Q. Wang, *ACS Sustainable Chem. Eng.*, 2022, **10**, 7216–7222; (*b*) A. Metawea, R. Soto, M. Khraisheh, G. Walker and A. B. Albadarin, *Powder Technol.*, 2024, **437**, 119558.

34 (*a*) D. E. Crawford, L. A. Wright, S. L. James and A. P. Abbott, *Chem. Commun.*, 2016, **52**, 4215–4218; (*b*) H. Taheri, M. Hietala, T. Suopajärvi, H. Liimatainen and K. Oksman, *ACS Sustainable Chem. Eng.*, 2021, **9**, 883–893.

35 D. E. Crawford, C. K. G. Miskimmin, A. B. Albadarin, G. Walker and S. L. James, *Green Chem.*, 2017, **19**, 1507–1518.

36 S. Arfelis, A. I. Martín-Perales, R. Nguyen, A. Pérez, I. Cherubin, C. Len, I. Malpartida, A. Bala and P. Fullana-i-Palmer, *Heliyon*, 2024, **10**, e34655.

37 C. Marschik, W. Roland and T. A. Osswald, *Polymers*, 2022, **14**, 875.

38 K. J. Ardila-Fierro and J. G. Hernández, *ChemSusChem*, 2021, **14**, 2145–2162.

39 B. M. Sharma, R. S. Atapalkar and A. A. Kulkarni, *Green Chem.*, 2019, **21**, 5639–5646.

40 (*a*) V. Pandey and J. M. Maia, *J. Appl. Polym. Sci.*, 2021, **138**, 49716; (*b*) N. D. Polychronopoulos, K. Moustris, T. Karakasidis, J. Sikora, V. Krasinskyi, I. E. Sarris and J. Vlachopoulos, *Polym. Eng. Sci.*, 2025, 27170.

41 C. Verma, D. S. Chauhan, R. Aslam, P. Banerjee, J. Aslam, T. W. Quadri, S. Zehra, D. K. Verma, M. A. Quraishi, S. Dubey, A. AlFantazi and T. Rasheed, *Green Chem.*, 2024, **26**, 4270–4357.

42 (*a*) S. S. Karade, S. Lalwani, J.-H. Eum and H. Kim, *Sustainable Energy Fuels*, 2020, **4**, 3066–3076; (*b*) M. H. Shafie, R. Yusof and C.-Y. Gan, *J. Mol. Liq.*, 2019, **288**, 111081.

43 N. Azizi and M. Edrisi, *Monatsh. Chem.*, 2015, **146**, 1695–1698.

44 D. D. Pathak and V. Grover, in *Handbook on Synthesis Strategies for Advanced Materials*, ed. A. K. Tyagi and R. S. Ningthoujam, Springer Singapore, Singapore, 2021, pp. 657–682.

45 C. Chuang and M. Lien, *Eur. J. Org Chem.*, 2004, **2004**, 1432–1443.

46 H. Patil, S. K. Vemula, S. Narala, P. Lakkala, S. R. Munnangi, N. Narala, M. O. Jara, R. O. Williams, H. Terefe and M. A. Repka, *AAPS PharmSciTech*, 2024, **25**, 37.

47 V. Štrukil and D. Margetic, in *Sustainable Organic Synthesis*, ed. S. Protti and A. Palmieri, Royal Society of Chemistry, Cambridge, 2021, pp. 181–211.

48 D. W. Londe, R. Dwayne Elmore, C. A. Davis, S. D. Fuhlendorf, B. Luttbeg and T. J. Hovick, *Ecosphere*, 2020, **11**, e03290.

49 K. J. Crowley and G. Zografi, *J. Pharm. Sci.*, 2002, **91**, 492–507.

50 L. E. Wenger and T. P. Hanusa, *Chem. Commun.*, 2023, **59**, 14210–14222.

51 T. Sun, W. Zhang, C. Zong, P. Wang and Y. Li, *J. Pept. Sci.*, 2010, **16**, 364–374.

52 Z. Lu, G. B. Hammond and B. Xu, *Org. Biomol. Chem.*, 2020, **18**, 6849–6852.